Preprint, 11th IFAC Symposium on Dynamics and Control of Process Systems,
including Biosystems
June 6-8, 2016. NTNU, Trondheim, Norway

Online Optimal Experiment Design: Reduction of the Number of Variables ⋆

Roberto Lemoine-Nava, * **Sebastian F. Walter,** **
Stefan Körkel, ** **Sebastian Engell** *

* *Process Dynamics and Operations Group, Technische Universität Dortmund, Emil-Figge-Str. 70, 44227 Dortmund, Germany (Tel: +49 231 755-5809; e-mail: Roberto.Lemoine@bci.tu-dortmund.de).*
** *Interdisciplinary Center for Scientific Computing, Universität Heidelberg, Im Neuenheimer Feld 368, 69120 Heidelberg, Germany*

Abstract: In this work, a method for reducing the number of degrees of freedom in online optimal dynamic experiment design problems for systems described by differential equations is proposed. The online problems are posed such that only the inputs which extend an operation policy resulting from an experiment designed offline are optimized. This is done by formulating them as multiple experiment designs, considering explicitly the information of the experiment designed offline and possible time delays unknown *a priori*. The performance of the method is shown for the case of the separation of isopropanolol isomers in a Simulated Moving Bed plant.

Keywords: Optimal experiment design; Large scale systems; Decomposition methods; Partial differential equations; Time delay; Chromatography; Simulated Moving Bed process

1. INTRODUCTION

First principles mathematical models are of paramount importance for purposes such as optimization and control of systems of practical relevance (chemical, biological, mechanical, etc.). Typically, the models are parametrized by means of experiments in laboratory or in small scale plants. However, the parameters in the real plant might deviate from the values determined from such experiments due to factors such as fouling and material aging, just to mention a few. Process monitoring techniques provide a solution for detecting changes in the parameters which are critical for predicting the key performance indicators of the system. These techniques require that the measurements obtained from the process during its operation contain enough information to estimate the parameters with an acceptable accuracy. This can be achieved by means of Optimal Experiment Design (OED) (Körkel (2002)). Different approaches have been proposed for the application of OED methods online, oriented either to system identification (see e.g. Gevers et al. (2011) and references therein) or to an improved estimation of the parameters of a physically motivated process model. In this category, a recurring approach is to perform the OED online in an adaptive moving horizon fashion, in which only the first element of the optimal control sequence is applied to the system, followed by a parameter estimation step, and the procedure is repeated either indefinitely or until the end of the experiment (Zhu and Huang (2011), Qian et al. (2014), Lucia and Paulen (2014)). A common aspect of the approaches proposed in all of the aforementioned references is that the online experiment designs are reoptimized between sampling instants. In the case studies treated by the authors this is an acceptable assumption because in all cases, systems described by low order dynamic models were considered. However, this might not be realistic if the models have a much larger order, such as in the case of plant-wide models of complete processes, or of systems emerging from discretized partial differential equations (PDE). The complexity of online OED task increases further if the amount of degrees of freedom (DOF) is large.

In this contribution, a method for significantly reducing the amount of the degrees of freedom in the online experiment design optimization problem is proposed. The paper is structured as follows: First, a general description of the OED problem is provided. Next, the difficulties involved in the OED are explained, and the proposed scheme is presented. Finally, the performance of the scheme is demonstrated by its application to the separation of isopropanolol isomers in a Simulated Moving Bed (SMB) plant.

2. OPTIMAL DYNAMIC EXPERIMENT DESIGN

The objective of the optimal dynamic experiment design (ODED) is to determine a set of control inputs which excite a dynamic system such that the noisy measurements of the resulting response provide a maximum amount of information to estimate the parameters of a model, which is assumed to be structurally correct, with the narrowest possible confidence intervals. If m variables described by the model can be measured, and if the measurents are corrupted with Gaussian noise with zero mean and with standard deviations $\underline{\sigma} = [\sigma_1, ..., \sigma_m]$, the parameter estimates $\underline{\hat{p}}$ of the model can be obtained by solving the constrained least-squares estimation problem (1):

⋆ The research leading to these results has received funding from the ERC Advanced Investigator Grant MOBOCON under the grant agreement No. 291458.

$$\min_{\hat{p}} \frac{1}{2}\sum_{i=1}^{m}\sum_{n=1}^{N}\left(\frac{y_i\left(t_n\right)-\hat{y}_i\left(\underline{\hat{x}}\left(t_n,\underline{\hat{x}}_0,\underline{u},\underline{\hat{p}}\right)\right)}{\sigma_i}\right)^2 \quad (1)$$

$$\text{s.t. } \frac{d\underline{\hat{x}}}{dt}=\underline{f}\left(t,\underline{\hat{x}},\underline{u},\underline{\hat{p}}\right), \qquad \underline{\hat{x}}\left(t=0\right)=\underline{\hat{x}}_0, \quad (2)$$

$$\underline{\hat{y}}=\underline{h}\left(\underline{\hat{x}},\underline{u},\underline{\hat{p}}\right) \quad (3)$$

$$\underline{0}\leq\underline{g}\left(\underline{\hat{x}}\left(t_1,\underline{\hat{x}}_0,\underline{u},\underline{\hat{p}}\right),\ldots,\underline{\hat{x}}\left(t_N,\underline{\hat{x}}_0,\underline{u},\underline{\hat{p}}\right)\right) \quad (4)$$

where $\underline{f}$, $\underline{h}$ and $\underline{g}$ are vector functions which define the system dynamics, the measurements and the constraints of the problem, respectively. $\underline{\hat{y}}_i\left(t\right)$ and $\underline{y}_i\left(t\right)$ are the system responses predicted by the model and measured at the time instants $t=\left[t_1,t_2,...,t_N\right]^T$. The predicted responses $\underline{\hat{y}}_i\left(t\right)$ depend on the estimated values of the states $\underline{\hat{x}}$, the state estimates at the beginning of the time horizon $\underline{\hat{x}}_0$, the control inputs $\underline{u}$ and the parameter estimates $\underline{\hat{p}}$ themselves. The measured responses $\underline{y}_i\left(t\right)$ depend on the current and on the initial states of the plant ($\underline{x}$ and $\underline{x}_0$), on the control inputs $\underline{u}$, on the real parameters of the plant $\underline{p}$ and on the measurement noise. Under these assumptions, the measurents are normally distributed random variables:

$$y_i\sim\mathcal{N}\left(\hat{y}_i\left(\underline{x}\left(t_i,t_0,\underline{x}_0,\underline{p},\underline{u}\right)\right),\sigma_i^2\right) \quad (5)$$

The confidence intervals of the estimates $\hat{p}$ are related to the covariance matrix of the parameters $\underline{\mathbf{C}}$, defined as:

$$\underline{\mathbf{C}}=\underline{J}^{+}\begin{pmatrix}\underline{I} & \underline{0}\\ \underline{0} & \underline{0}\end{pmatrix}\underline{J}^{+^T}, \quad (6)$$

where

$$\underline{J}^{+}=\begin{pmatrix}\underline{I} & \underline{0}\end{pmatrix}\begin{pmatrix}\underline{J}_1^T\underline{J}_1 & \underline{J}_2^T\\ \underline{J}_2 & \underline{0}\end{pmatrix}^{-1}\begin{pmatrix}\underline{J}_1^T & \underline{0}\\ \underline{0} & \underline{I}\end{pmatrix}. \quad (7)$$

Here, $\underline{J}_1$ is the Jacobian of the model of the measurements with respect to the parameters and to the initial states:

$$\underline{J}_1=\begin{pmatrix}\frac{w_1}{\sigma_1}\frac{\partial\hat{y}_1}{\partial\underline{\hat{p}}} & \cdots & \frac{w_1}{\sigma_1}\frac{\partial\hat{y}_1}{\partial\underline{\hat{x}}_0}\\ \vdots & \ddots & \vdots\\ \frac{w_m}{\sigma_m}\frac{\partial\hat{y}_m}{\partial\underline{\hat{p}}} & \cdots & \frac{w_m}{\sigma_m}\frac{\partial\hat{y}_m}{\partial\underline{\hat{x}}_0}\end{pmatrix}=\left(\underline{J}_1^{\hat{p}}\mid\underline{J}_1^{\hat{x}_0}\right) \quad (8)$$

where w_i are the weights of the measurements, which can also enter as degrees of freedom in the optimization. $\underline{J}_2$ is the Jacobian of the constraints $\underline{g}$ with respect to $\underline{\hat{p}}$, i.e. $\underline{J}_2=\left(\mathrm{d}\underline{g}/\mathrm{d}\underline{\hat{p}}\mid\mathrm{d}\underline{g}/\mathrm{d}\underline{\hat{x}}_0\right)=\left(\underline{J}_2^{\hat{p}}\mid\underline{J}_2^{\hat{x}_0}\right)$ (Körkel (2002)).

The objective function to be minimized is a scalar criterion related to the measure of the covariance matrix $\Phi\left(\underline{\mathbf{C}}\right)$ (such as its trace, determinant, or largest eigenvalue), which is directly related to the confidence intervals.

3. DIFFICULTIES OF THE OED FOR LARGE SCALE DYNAMIC SYSTEMS WITH TIME DELAYS

In the design of experiments for dynamic systems, the time needed to see the effect of the control inputs on the measurements must be accounted for. For systems with time delays, this can result in large time horizons which must be taken into account in the experiment design. Additionally, if the model of the system is highly parameterized, a relatively large amount of measurements must be considered to get enough information to estimate the parameters reliably.

In the OED problem, the first and second derivatives of the model of the system and of the constraints of the problem with respect to the state variables, the parameters and the inputs are necessary in order to evaluate the objective function, as well as if a gradient-based algorithm is used. Computing the derivatives at each iteration becomes slow and memory consuming as the amount of measurements and of inputs discretized in time increases. If the number of states and of parameters is large, the evaluation of the objective function becomes very time consuming, leading to prohibitively large times per iteration during the optimization. Additionally, increasing the amount of DOF of the optimization by choosing finer time discretizations for the inputs leads to a slower convergence of the problem.

4. DESCRIPTION OF THE PROPOSED METHOD

The proposed ODED scheme consists of a decomposition of the original optimization problem into a series of reduced OED problems with considerably less measurements and DOF. The solutions of the reduced problems extend a control input sequence available from a prior experiment design, that from this point on will be referred as the *past experiment*, and which is assumed to be available from e.g. a start-up experiment or from another scenario in which the optimization time is not critical. It will be assumed that the time horizon of the past experiment is divided into K segments of equal length Δt. Within these segments, each control input i has N_u^i different parametrizations, and N_y^j samples of the measured quantity j are taken. Assume also that the time horizon of the past and of the online experiments have the same length, and that the time horizon of the online experiment is one Δt segment ahead of the time horizon of the past experiment. Thus, if the horizon of the past experiment starts at t_0, the horizon of the past and of the online experiments are $[t_0,\ t_{K\Delta t}]$ and $[t_{\Delta t},\ t_{(K+1)\Delta t}]$, and the inputs of the past experiment corresponding to the interval $[t_0,\ t_{\Delta t})$ are actually applied to the system.

In order to reduce the number of degrees of freedom corresponding to the control inputs in the online optimization problem, constraints are imposed on the inputs within the interval $[t_{\Delta t},\ t_{K\Delta t})$ to be the same as in the past experiment. In this way, the only degrees of freedom left in the online problem are the the control inputs in the interval $[t_{K\Delta t},\ t_{(K+1)\Delta t}]$, which are intended to extend the input sequence of the past experiment. We call this interval the *optimization horizon*. If the system shows time delays in its input-output behavior, the inputs applied close to the end of the time horizon do not influence the measured variables anymore, and thus do not contribute to minimizing the objective function. To overcome this problem, it is possible to define an extended optimization horizon $[t_{(K-N_{opt}+1)\Delta t},\ t_{(K+1)\Delta t}]$ with $N_{opt}\in\{1,2,...,K\}$. This implies letting the control inputs of the online experiment in the interval $[t_{(K-N_{opt}+1)\Delta t},\ t_{(K)\Delta t})$ free. Notice that the inputs in the interval $[t_{0+\Delta t},\ t_{(K-N_{opt}+1)\Delta t})$ of the online experiment only simulate the system. The structure of the horizon of the online optimization resembles the time delay compensation concept proposed in Ellis and Christofides (2015) for economic predictive control. Forgione et al. (2014) proposed a similar concept in the OED context, but solved the problem with a combinatorial approach.

To reduce the number of measurements in the online optimization, only measurements in the interval $(t_{K\Delta t},\ t_{(K+1)\Delta t})$ are taken into account for the OED. However, in order for the online experiment to further improve the results of the past experiment, it is necessary to include the measurement information considered for the design of the latter in the online optimization. This can be done by replacing the covariance matrix $\underline{J}_1$ in Eq. 7, which corresponds to the online problem alone, by an extended covariance matrix $\underline{\tilde{J}}_1$ which condenses the covariances of the online and of the past experiments, namely $\underline{J}_{1,O}$ and $\underline{J}_{1,P}$, as shown in Eq. 9. The blocks $J_{1,i}^{\hat{p}}$ and $J_{1,i}^{\hat{x}_0}$, with $i = \{O, P\}$, have the same definition as in Eq. 8.

$$\underline{\tilde{J}}_1 = \begin{pmatrix} \underline{J}_{1,P}^{\hat{p}} & \underline{J}_{1,P}^{\hat{x}_0} & \underline{0} \\ \\ \underline{J}_{1,O}^{\hat{p}} & \underline{0} & \underline{J}_{1,O}^{\hat{x}_0} \end{pmatrix} \tag{9}$$

We define the *measurement bank* of an experiment as the set of measurements considered for the design of the experiment. Once the online problem has been solved, the inputs in the interval $[t_{(K-N_{opt}+1)\Delta t},\ t_{K\Delta t})$ of the past experiment are substituted by the inputs of the online experiment corresponding to the same interval if $N_{opt} > 1$, and the past experiment is extended by the inputs of the online experiment in the interval $[t_{K\Delta t},\ t_{(K+1)\Delta t}]$. Additionally, the measurement bank of the past experiment is extended with the measurement bank of the online experiment. For the next online optimization, the past experiment is shifted one Δt segment in order to avoid it from growing indefinitely, and the procedure is repeated. Finally, the measurements corresponding to time instants in the past of the shifted past experiment are removed from its measurement bank.

The procedure is illustrated in Figure 1 for a system which is assumed to have a time delay of two Δt segments. A parametrization of the online experiments with one piecewise constant input i and two samples of the measured quantity j per Δt segment and an optimization horizon of $3\Delta t$ (i.e. $N_u^i = 1$, $N_y^j = 2$ and $N_{opt} = 3$), and a time horizon of $7\Delta t$ for both online and past experiments have been considered. Figure 1a shows the initial experiment designed offline assuming ten measurements evenly distributed in the time horizon past the $2\Delta t$ time delay segments, i.e. with a measurement bank with an initial time horizon length of $5\Delta t$. Figure 1b shows the first online experiment, for whose design the offline experiment is treated as the past experiment, represented by the solid lines. The online optimization is started at the initial time t_0, and its solution, represented by the dashed lines, is assumed to be available after Δt time units. The subsequent experiments are shown in Figures 1c and 1d, where it can be seen that the inputs of the shifted past experiment are substituted by the optimal inputs from the online experiments, and that the length of the horizon of the measurement bank of the past experiment increases from $5\Delta t$ to $6\Delta t$ and $7\Delta t$, respectively. Finally, Figure 1e shows the removal of past measurements behind the time horizon of the past experiment from its measurement bank.

Besides the reduction of the degrees of freedom of the online optimization problem, the proposed approach has the advantage that, in theory, arbitrarily many measurements

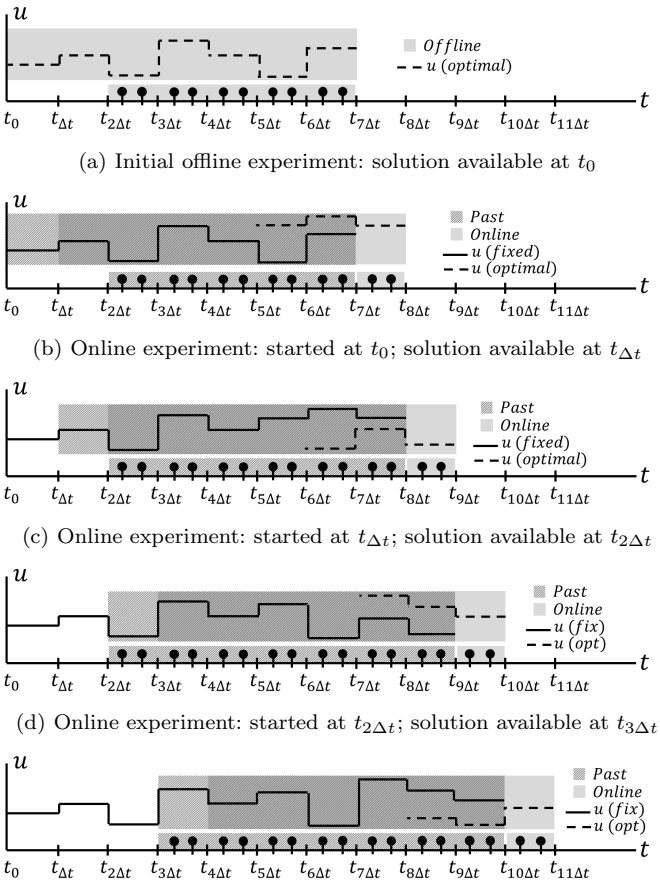

(a) Initial offline experiment: solution available at t_0

(b) Online experiment: started at t_0; solution available at $t_{\Delta t}$

(c) Online experiment: started at $t_{\Delta t}$; solution available at $t_{2\Delta t}$

(d) Online experiment: started at $t_{2\Delta t}$; solution available at $t_{3\Delta t}$

(e) Online experiment: started at $t_{3\Delta t}$; solution available at $t_{4\Delta t}$

Fig. 1. Schematic representation of the online experiment design method for four consecutive Δt segments.

can be contained in the measurement bank of the past experiment, depending on the length of the time horizon of the experiments. This can be used for increasing the information content available for the online experiment designs, thus improving the quality of their solutions. As the inputs of the past experiment are fixed, its covariance information (i.e. the blocks $J_{1,P}^{\hat{p}}$ and $J_{1,P}^{\hat{x}_0}$ of the extended covariance matrix $\underline{\tilde{J}}_1$) must be evaluated only once for each online experiment, prior to the onset of the optimization. Thus, the only price to pay for counting on a large measurement bank is a larger time for the integrating the system and the evaluation of the sensitivities with respect to the states and parameters, plus an increment of the memory requirements due to the simultaneous treatment of both experiments. Additionally, the matrix $\underline{\tilde{J}}_1$ can be efficiently calculated due to its structure (Körkel (2002)).

The objective function and constraints specific to the proposed method are:

$$\min_{\underline{u}_O}\ \Phi\left(\underline{\mathbf{C}}\left(\underline{\tilde{J}}_1, J_{2,O}\right)\right) \tag{10}$$

$$\text{s.t.} \quad \underline{0} = \underline{u}_O(t) - \underline{u}_P(t), \quad t_{\Delta t} \le t < t_{(K-N_{opt}+1)\Delta t} \tag{11}$$

where $\underline{u}_O$ and $\underline{u}_P$ are the inputs of the online and the past experiments, respectively.

5. CASE STUDY: THE SMB PROCESS

The SMB is a continuous chromatographic process. The continuous operation is achieved by approximating a counter-current flow between the fluid mixture and the solid. The SMB process consists of a series of chromatographic columns connected in a ring. The mixture and the solvent are fed continuously at specific nodes between columns. Similarly, the resulting purified components are removed continuously from the plant at the extract (rich in the more strongly adsorbed component A) and at the raffinate (rich in the less strongly adsorbed component B) ports, which typically count with sensors for the product concentrations. The feed and product ports are moved periodically by one column in the direction of the liquid flow. A SMB plant is divided in four zones: in Zone I (between the solvent and extract ports) the component A is recovered and the solid is regenerated; in Zone II (between the extract and feed ports) the component B is desorbed; in Zone III (between the feed and raffinate ports) the component A is adsorbed and the component B is recovered; and in Zone IV (between the raffinate and solvent ports) the component B is adsorbed and the solvent is regenerated. The process is shown in Figure 2.

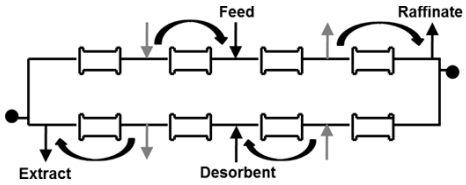

Fig. 2. Schematic representation of the SMB process.

5.1 Process model

The columns in the SMB plant are modelled by the General Rate Model (GRM) (Schmidt-Traub (2012)). The GRM consists of equations for the concentrations of component i in the liquid in the bulk phase ($C^{b,i}$) in the axial direction z (Eq. 12), and in the pores of the adsorbent ($C^{p,i}$) in the particle radial direction r (Eq. 13), with the boundary conditions shown in Eqs. 14 and 15:

$$\begin{aligned}\frac{\partial C^{b,i}}{\partial t} &= D^i_{ax}\frac{\partial^2 C^{b,i}}{\partial z^2} - v\frac{\partial C^{b,i}}{\partial z} \qquad (i=\{A,B\}) \\ &\quad - \left(\frac{1-\epsilon_b}{\epsilon_b}\right)\frac{3k^i_l}{r_p}\left(C^{b,i} - C^{p,i}|_{r=r_p}\right).\end{aligned} \tag{12}$$

$$(1-\epsilon_b)\frac{\partial q^i}{\partial t} + \epsilon_p\frac{\partial C^{p,i}}{\partial t} = \epsilon_p D^i_p \frac{1}{r^2}\frac{\partial}{\partial r}\left(r^2\frac{\partial C^{p,i}}{\partial r}\right). \tag{13}$$

$$\left.\frac{\partial C^{b,i}}{\partial z}\right|_{z=L} = 0; \quad \left.\frac{\partial C^{b,i}}{\partial z}\right|_{z=0} = \frac{v}{D^i_{ax}}\left(C^{b,i} - C^{b,i}_{in}\right). \tag{14}$$

$$\left.\frac{\partial C^{p,i}}{\partial r}\right|_{r=0} = 0; \quad \left.\frac{\partial C^{p,i}}{\partial r}\right|_{r=r_p} = \frac{k^i_l}{\epsilon_p D^i_p}\left(C^{b,i} - C^{p,i}|_{r=r_p}\right). \tag{15}$$

In the model, D^i_{ax} is the axial dispersion coefficient (see Schmidt-Traub (2012)), D^i_p is particle diffusion coefficient, k^i_l is the mass transfer coefficient of component i, r_p is the particle radius, v is interstitial velocity, and ϵ_b and ϵ_p are the bulk and particle porosities. It is assumed that the concentrations of the component i in the liquid at the particle pores and at the surface of the adsorbent (q^i) are in equilibrium, described by adsorption isotherms, which depend on the chromatographic system.

The material balances at the interconnection nodes are:

$$0 = -Q_I + Q_{IV} + Q_{De} \tag{16a}$$
$$0 = -Q_{II} + Q_I - Q_{Ex} \tag{16b}$$
$$0 = -Q_{III} + Q_{II} + Q_F \tag{16c}$$
$$0 = -Q_{IV} + Q_{III} - Q_{Ra} \tag{16d}$$
$$0 = -C^{b,i}_{out,IV}Q_{IV} + C^{b,i}_{in,I}Q_I \tag{16e}$$
$$0 = -C^{b,i}_{out,II}Q_{II} - C^i_F Q_F + C^{b,i}_{in,III}Q_{III}, \tag{16f}$$

where $i=\{A,B\}$, and Q_j is the flow rate of zone j.

Finally, the purity of the species i at the product port j can be calculated as described in Eq.

$$Pu^j_i = \frac{m^j_i}{m^j_A + m^j_B}, \qquad i=\{A,B\},\ j=\{Ex,Ra\} \tag{17}$$

where m^j_i is the accumulated mass of species i at port j.

5.2 OED for improved estimation of adsorption isotherm parameters in the SMB process

The parameters of the adsorption isotherms are usually estimated from measurements in laboratory scale columns (Schmidt-Traub (2012)). The estimated values can differ in reality from the ones of the SMB plant. Even small heterogeneities in the packing of the columns can reflect on the measurements at the product ports (Lemoine-Nava and Engell (2014)). However, in general it is not possible to know *a priori* which members of the parameter set must be tracked, especially in the case of highly parametrized isotherms. The estimation is further complicated by the fact that it is not possible to obtain permanently measurements from all the columns due to the switching of the sensors at the product ports.

We propose to use the ODED method introduced in this work to improve the estimation of the isotherm parameters of the individual columns. We impose a constraint only on the purity of the mixture component of interest at the port where it is enriched in order to enable the simultaneous detection of both components in the sensor at the other port. This is to allow the estimation of isotherm parameters representing the interaction between the mixture components, which appear in many types of nonlinear adsorption isotherms. The treatment of the second product is out of the scope of this work. We choose the flow rates of the desorbent, extract, feed and recycle pump (Q_D, Q_E, Q_F and Q_{Re}), the period length (i.e. time between port switches) τ and the feed concentration C_F as the degrees of freedom (DOF). The flow rates are substituted as DOF by the so-called β-factors to improve the numerical tractability of the problem:

$$\begin{aligned}\overline{H}_A\beta_I &= \frac{Q_I}{Q_s} - \frac{\epsilon_b}{1-\epsilon_b}, & \overline{H}_B\beta_{II} &= \frac{Q_{II}}{Q_s} - \frac{\epsilon_b}{1-\epsilon_b}, \\ \frac{\overline{H}_A}{\beta_{III}} &= \frac{Q_{III}}{Q_s} - \frac{\epsilon_b}{1-\epsilon_b}, & \frac{\overline{H}_B}{\beta_{IV}} &= \frac{Q_{IV}}{Q_s} - \frac{\epsilon_b}{1-\epsilon_b}, \\ Q_s &= (1-\epsilon_b)\frac{\pi D^2 L}{4}\frac{1}{\tau},\end{aligned} \tag{18}$$

where $\overline{H}_A$ and $\overline{H}_B$ are the average Henry parameters of the plant. We choose the trace of the covariance matrix as

the objective function in Eq. 10 (i.e. $\Phi(\underline{\mathbf{C}}) = tr(\underline{\mathbf{C}})$), with $\underline{u}_O = \{\beta_I, \beta_{II}, \beta_{III}, \beta_{IV}, \tau, C_F\}$, subject to the constraints (11), the box constraints of the external flow rates:

$$\begin{aligned} 1.7 \cdot 10^{-4} \leq Q_F \leq 0.08 \text{ cm}^3\text{s}^{-1} \\ 1.7 \cdot 10^{-4} \leq Q_D \leq 0.33 \text{ cm}^3\text{s}^{-1} \\ 1.7 \cdot 10^{-4} \leq Q_E \leq 0.33 \text{ cm}^3\text{s}^{-1} \end{aligned} \quad (19)$$

and the constraint on the purity of the product of interest:

$$\underline{0} \leq Pu_i^j - Pu_{i,min}^j, \quad i = \{A \vee B\},\ j = \{Ex \vee Ra\} \quad (20)$$

Including the feed concentration C_F among the degrees of freedom is interesting because the distance between the feed stream and the port sensors is relatively large, originating an inherent delay in the input-output behavior.

6. RESULTS

To test the performance of the proposed scheme, the case of the separation of an isopropanolol racemic mixture in a six-column SMB plant with a 1/2/2/1 zone distribution has been considered. The adsorption behavior of the mixture is described by an extended Langmuir isotherm:

$$q^i = H_1^i C^{p,i} + \frac{H_2^A C^{p,i}}{1 + K^A C^{p,A} + K^B C^{p,B}}, \quad i = \{A, B\} \quad (21)$$

The isotherm has six parameters, leading to 36 individual column parameters. The PDE system of the GRM has been discretized with the Finite Element Method in the fluid phase, and with Orthogonal Collocation in the solid phase (Lemoine-Nava and Engell (2014)). For each column, 17 nodes were chosen for the fluid phase, and 1 collocation point for the pore phase, leading to 408 states for the discretized system. The nominal isotherm parameters are H_1^A=2.68, H_1^B=2.2, H_2^A=0.9412, H_2^B=0.4153, K^A=340 cm^{3}g^{-1} and K^B=262 cm^{3}g^{-1}. The rest of the parameters are k_l^A=5.6 s^{-1}, k_l^B=3.3 s^{-1}, $\epsilon_b = 0.4, \epsilon_p$=0.5, D_p^i=0.001 cm^2 s^{-1} and r_p=0.002 cm. A column length L=10 cm and diameter D=1 cm, a viscosity ν=6.85x10^{-4} P and a density ρ = 1.0 g cm^{-3} were specified.

Following the nomenclature in Section 4, the Δt segments for the experiments have been considered to have a length equal to one normalized period. The parametrization chosen for online OED scheme is $N_{opt} = 5\Delta t$, with 21 measurement samples per period, i.e. $N_y^j = 21$. It has been assumed that the SMB plant has a sensor permanently at the outlet of the last column of the plant and at the product ports. The relatively large value chosen for N_{opt} is to counteract time delays in the input-output behavior of the plant. It has been assumed that the flow rates only change between periods, and that the feed concentrations can change up to four times per period by means of dilution, i.e. $N_u^{Q_{Re}}$=$N_u^{Q_D}$= $N_u^{Q_E}$=$N_u^{Q_F}$=N_u^{τ}=1 and $N_u^{C_F} = 4$. The online and "past" experiments were assumed to have a time horizon of 12 periods. The OED scheme was simulated for a total time horizon of 54 periods. A minimum purity of 90% of the component B at the raffinate port has been specified.

The extension reVPLAN (Walter et al. (2014)) of the software tool VPLAN (Körkel (2002)) was used for solving the OED problems. VPLAN supports the design of experiments considering information from past experiments as described in Eq. 9. The optimization problems were solved with IPOPT (Wächter and Biegler (2006)). The warm start capabilities of IPOPT were used for the online optimization problems. The model of the SMB process was implemented using banded storage in order to exploit the structure of the spatial discretization of the PDE system.

Figure 3 shows the input sequences applied to the plant, resulting from the optimal experiments. The first "past" experiment is the result of an offline optimization of the SMB plant that is initially empty. For the offline optimization a measurement bank with an initial length of $6\Delta t$ (with a total of 126 measurement samples) was chosen. A large effort was necessary to find a suitable initial parametrization which resulted in convergence of the optimizer, and that it takes more than 40 minutes for the optimization to find the solution in a computer with an Intel(R) Xeon processor at 2.50 GHz with eight cores. The first online experiment reoptimizes the input sequence calculated by the offline "past" experiment starting from the 8th period. It can be seen that the flow rates show aggressive changes during the whole operation horizon, showing that the proposed OED scheme manages to introduce excitation to the process as long as it is active. The period length behaves less abruptly. It can also be seen that the feed concentration changes significanlty during the operation horizon past the period corresponding to the "past" offline experiment. This is interesting, because it suggests that our scheme manages to use this variable for introducing excitation into the system despite of the large input-output delay. The concentrations measured at the extract and the raffinate ports are shown in Figure 4. It can be seen that the operation policy calculated with the online experiment designs allows to fulfill the constraints imposed on the purity of the raffinate.

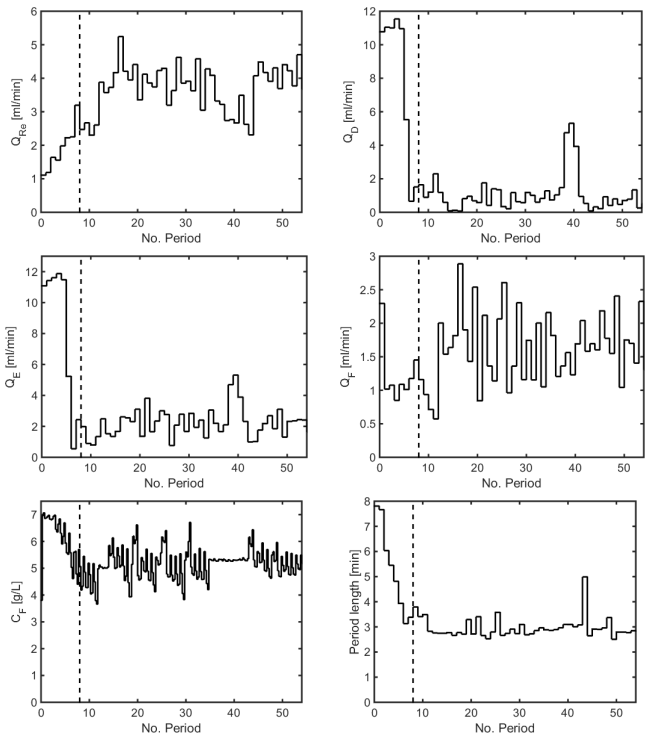

Fig. 3. Optimal dynamic experiment for the estimation of isotherm parameters of the individual columns of the SMB plant. The inputs starting from the 8th period are calculated with online experiments.

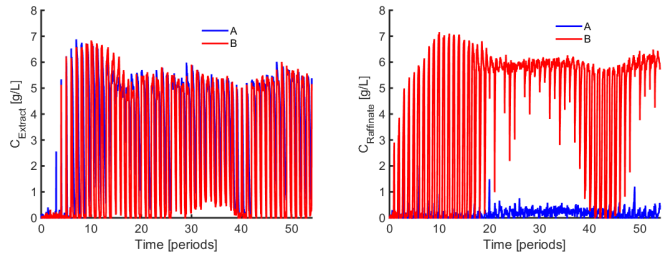

Fig. 4. Concentrations measured at the extract (left) and raffinate (right) ports.

Finally, the evolution of the expected standard deviations of the parameters of columns 2 and 6 is shown in Figure 5. The standard deviations of the parameters of the other columns behave similarly and are not shown due to space limitations. It can be seen that the parameters H_1^A and H_1^B of all the columns have very small standard deviations along the whole time horizon, and thus are easy to estimate. This is consistent with the fast convergence rates observed in Lemoine-Nava and Engell (2014) for the estimation of these parameters for the same chromatographic system, but no OED was performed in that work. The parameters H_2^A, H_2^B, K_A and K_B of column 2 show a large increment in their expected standard deviations after approximately 30 periods. Afterwards, the online experiment design scheme manages to keep the standard deviations of H_2^A and H_2^B in a range of 25 to 50% and 30 to 65%, while for the interaction coefficients K_A and K_B the expected standard deviations are between 50 to 80% and 45 to 85%. An improvement is observed for the standard deviations of the parameters of column 6. For H_2^A and H_2^B, they are expected to be in a range of 10 to 30% and 20 to 40%, while for the case of K_A and K_B, they are expected to be between 30 to 50% and 30 to 55%. The improved standard deviations of the parameters of column 6 can be attributed to the additional measurement information that the column obtains from the fixed sensor at its outlet.

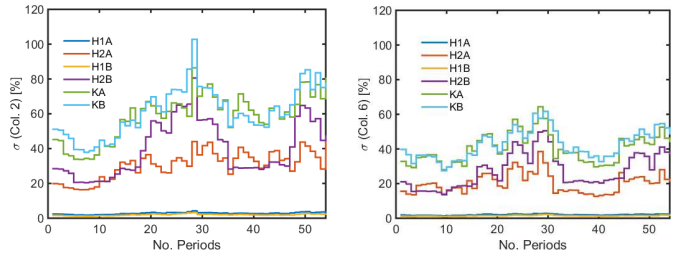

Fig. 5. Evolution of the expected parameter standard deviations of columns 2 (left) and 6 (right).

Times between 4 and 14 minutes per online optimization in a computer with an Intel(R) *i*7 processor at 3.60 GHz with eight cores were reported by IPOPT for this case study. However, this time is counted past the initial evaluation of the covariance matrices prior to the onset of the optimization iterations. The computation time is heavily dependent on many factors such as the tolerances used for integrating the system and evaluating sensitivities, the tolerance chosen for the optimizer, etc. Further research should be done in order to give this scheme full real-time capabilities. However, our method has shown that it can significanlty decrease the computation times obtained otherwise for experiments with many measurements and large time horizons.

7. CONCLUSIONS

In this work, a new method for reducing the amount of DOF in online Optimal Experiment Designs was introduced. The approach implies the decomposition of the full OED problem into a series of smaller OED problems, taking explicitly into account the information from past experiments in the design optimization. The approach allows to significantly reduce the computation time for the solution of the optimizations. The method was applied for the online OED for estimating the individual column isotherm parameters in a SMB plant, and it managed to keep an online operation while respecting the imposed product quality constraints. To our best knowledge, this is the first work in which online OED is applied to a PDE system, and it is also the first one to use the feed concentration for the online optimization of SMB processes.

REFERENCES

M. Ellis, and P.D. Christofides. Economic model predictive control of nonlinear time-delay systems: closed-loop stability and delay compensation. *AIChE Journal*, Article in press. 2015.

M. Forgione, X. Bombois, P.M.J. Van den Hof, and H. Hjalmarsson. Experiment design for parameter estimation in nonlinear systems based on multilevel excitation. *Proc. European Control Conference*, 25–30, 2014.

M. Gevers, X. Bombois, R. Hildebrand, and G. Solari. Optimal experiment design for open and closed-loop system identification. *Communications in Information and Systems*, 11:197-224, 2011.

S. Körkel. *Numerische Methoden für optimale Versuchsplanungsprobleme bei nichtlinearen DAE-Modellen* Dr. rer. nat. Dissertation. Universität Heidelberg, 2002.

R. Lemoine-Nava, and S. Engell. Individual Column State and Parameter Estimation in the Simulated Moving Bed Process: an Optimization-based Method. *Proc. IFAC 19th World Congress*, 9376–9381, 2014.

S. Lucia, and R. Paulen. Robust nonlinear model predictive control of uncertainty via robust optimal experiment design. *Proc. IFAC 19th World Congress*, 1904–1909, 2014.

H. Schmidt-Traub, M. Schulte and A. Seidel-Morgenstern. *Preparative Chromatography,* 340–344. Wiley-VCH, Weinheim, 2012.

J. Qian, M. Nadri, P.D. Morosan, and P. Dufour. Closed loop optimal experiment design for on-line parameter estimation *Proc. European Control Conference*, 1813–1818, 2014.

S.F. Walter, A. Schmidt, and S. Körkel. Adjoint-based optimization of experimental designs with many control variables. *Journal of Process Control*, 24:1504-1515, 2014.

A. Wächter, and L.T. Biegler. On the implementation of a primal-dual interior point filter line search algorithm for large-scale nonlinear programming. *Mathematical Programming*, 106:25-57, 2006.

Y. Zhu, and B. Huang. Constrained receding-horizon experiment design and parameter estimation in the presence of poor initial conditions. *AIChE Journal*, 57: 2808-2820, 2011.